A Note on the Consensus Protocol with Some Applications to Agent Orbit Pattern Generation

Panagiotis Tsiotras and Luis I. Reyes Castro

Abstract We propose an extension to the standard feedback control for consensus problems for multi-agent systems in the plane. The proposed extension allows for a richer class of trajectories including periodic and quasi-periodic solutions, as well as agreement to consensus states outside the convex hull of the initial positions of the agents. We investigate in great detail the special case of three agents, which results in non-trivial geometric patterns described by ellipsoidal, epitrochoidal and hypotrochoidal curves.

1 A Generalized Consensus Protocol

Consensus problems have been originally used in distributed computing and management science and, most recently, have found extensive application in multi-agent, mobile network problems [12, 16]. In this paper we propose a generalization of the standard consensus algorithm which has been used extensively in the literature [13, 3, 11]. The proposed extension of the standard consensus protocol leads to the following advantages: first, it can be used to achieve consensus at points that do not necessarily belong to the convex hull of the initial conditions. This may be beneficial in case of obstacle avoidance or as part of deception strategies. Second, as shown in the second part of the paper, it can be utilized to generate intricate geometrical patterns of the agent paths. These paths can be useful for coordinated, distributed surveillance and monitoring applications.

Coordinated algorithms for network formations have appeared previously, for example, in [14, 15, 7] as well as in the work of Leonard and Sepulchre [9, 17, 18]. Therein the authors make use of geometric information to achieve specific formation

Panagiotis Tsiotras
School of Aerospace Engineering, Georgia Institute of Technology, Atlanta, GA 30332-0105, USA
Tel: +1-404-894-9526, Fax: +1-404-894-2760, e-mail: tsiotras@gatech.edu

Luis I. Reyes Castro
School of Aerospace Engineering, Georgia Institute of Technology, Atlanta, GA 30332-0105, USA, e-mail: nacho_reyes@gatech.edu

patterns. The control laws are at the acceleration level (e.g., [7, 18]), often derived from potential-like functions. Typically, these works focus on uni-directional ring communication topology, assuming identical control laws for each agent (e.g., as in cyclic pursuit) [14]. In [14] all-to-all communication and fixed ring topology is assumed for the graph resulting in a cyclic pursuit. The particular choice of the communication topology leads to a graph Laplacian which is a circulant matrix and the achievable formations are lines, circles or logarithmic spirals, similarly to the results of [9, 17, 18, 15].

The consensus control law proposed in the current paper cannot be readily derived from a scalar potential and its design is at the velocity level, similarly to the original consensus protocol. Depending on the gain matrices, the resulting paths may lead to more intricate *trochoidal* paths, as opposed to just straight lines, cycles and spirals. Using minimal assumptions we are thus able to generate geometric patterns of the agent trajectories that go beyond formation-type geometric models [20, 14, 9, 10, 15].

A New Consensus Protocol

Consider N agents in the plane, whose locations are given by the state variables $x_i \in \mathbb{R}^2$ for $i = 1,\dots,N$, satisfying the differential equations

$$\dot{x}_i = u_i, \qquad i = 1,\dots,N. \tag{1}$$

As usual, to this problem we associate a graph $\mathscr{G}$ that describes the communication topology between the agents. That is, $\mathscr{G}$ has N nodes and M edges (links), with each edge denoting knowledge of the relative position between the corresponding agents. Two nodes are neighbors in the graph $\mathscr{G}$ (hence connected by an edge) if and only if they can communicate with each other. Throughout the paper it will be assumed that the communication topology is fixed, that is, the neighbors of each node do not change as the agents move.

Define the incidence matrix $D \in \mathbb{R}^{N\times M}$ with elements

$$d_{ij} = \begin{cases} +1, & \text{if } i\text{th node is the head of } j\text{th edge,} \\ -1, & \text{if } i\text{th node is the tail of } j\text{th edge,} \\ 0, & \text{otherwise.} \end{cases} \tag{2}$$

To each edge we assign the difference (error) variable

$$z_k = \sum_{\ell=1}^{N} d_{\ell k} x_\ell = \begin{cases} x_i - x_j, & \text{if } i \text{ is the head,} \\ x_j - x_i, & \text{if } j \text{ is the head,} \end{cases} \tag{3}$$

where $z_k \in \mathbb{R}^2$ for $k = 1,\dots,M$. If the columns of D are linearly independent, that is, if the graph does not contain cycles, then the error variables z_k are linearly independent vectors [1]. Note also that the graph is connected if and only if $\operatorname{rank} D = N-1$ [13, 4]. Introducing the stack vector $x = \begin{bmatrix} x_1^\mathsf{T} & \cdots & x_N^\mathsf{T} \end{bmatrix}^\mathsf{T} \in \mathbb{R}^{2N}$, the

state equations (1) can be written compactly as

$$\dot{x} = u, \tag{4}$$

where $u = \begin{bmatrix} u_1^\intercal & \cdots & u_N^\intercal \end{bmatrix}^\intercal \in \mathbb{R}^{2N}$. We propose the control following law[1] for (1)

$$u_i = -\gamma_i \sum_{k=1}^{M} d_{ik} z_k + \beta_i \sum_{k=1}^{M} d_{ik} p_k, \quad i = 1, \ldots, N, \tag{5}$$

where $p_k \in \mathbb{R}^2$ such that $p_k^\intercal z_k = 0$, where $\gamma_i > 0$ and $\beta_i \in \mathbb{R}$. For instance, let $p_k \stackrel{\text{def}}{=} Sz_k$, $(k = 1, \ldots, M)$, where S is the skew symmetric matrix

$$S = \begin{bmatrix} 0 & -1 \\ 1 & 0 \end{bmatrix}. \tag{6}$$

Letting the stack vector $p = \begin{bmatrix} p_1^\intercal & \cdots & p_M^\intercal \end{bmatrix}^\intercal \in \mathbb{R}^{2M}$ yields, $p = (I_M \otimes S)z$, where $z = \begin{bmatrix} z_1^\intercal & \cdots & z_M^\intercal \end{bmatrix}^\intercal \in \mathbb{R}^{2M}$. The composite control law (5) then takes the form

$$u = -(\Gamma D \otimes I_2)z + (BD \otimes I_2)p = -(\Gamma D \otimes I_2)z + (BD \otimes S)z, \tag{7}$$

where $\Gamma = \operatorname{diag}(\gamma_1, \ldots, \gamma_N)$ and $B = \operatorname{diag}(\beta_1, \ldots, \beta_N)$. Note that the standard consensus algorithm results as a special case of (7) where $B = 0$.

Remark 1. The basic idea behind the control law (5) is the use of additional geometric information, inferred from the relative distance between the agent and its neighbors. Specifically, the second term in (5) is proportional to the direction which is *perpendicular* to the relative distance between the agent and its neighbors. In (7) this information is encoded via the multiplication of the error state with the skew-symmetric matrix S. This new skew-symmetric term provides additional flexibility in terms of the achievable final rendezvous points, as well as in terms of the resulting trajectories followed by the agents.

Remark 2. The proposed control law (7) has the same form as the one given in [1, Eq. (16)]. However, since the second term is (7) is not the gradient of a scalar function, it does not come from a potential, and hence (7) is more general than the family of control laws of [1]. The absence of a scalar potential is owing to the skew-symmetric term in (7) which introduces a circulation. In this sense, the control law (7) is akin to the gyroscopic control laws proposed in the robotics literature [6, 21, 19].

[1] The alternative control law $u_i = -\sum_{k=1}^{M} \gamma_k d_{ik} z_k + \sum_{k=1}^{M} \beta_k d_{ik} p_k$ which weights each edge separately could have been used in lieu of (5). The results of the paper remain essentially the same for the latter choice as well.

Consensus and Final Rendezvous Position

From (3) it can be easily shown that the error vector z can be written compactly as follows

$$z = (D^\mathsf{T} \otimes I_2)x. \tag{8}$$

The differential equation for x is therefore given by

$$\begin{aligned}\dot{x} &= -(\Gamma D \otimes I_2)(D^\mathsf{T} \otimes I_2)x + (BD \otimes S)(D^\mathsf{T} \otimes I_2)x \\ &= -\big((\Gamma D D^\mathsf{T}) \otimes I_2 - (BDD^\mathsf{T}) \otimes S\big)x \\ &= -\big((\Gamma L) \otimes I_2 - (BL) \otimes S\big)x,\end{aligned} \tag{9}$$

where $L \stackrel{\text{def}}{=} DD^\mathsf{T} \in \mathbb{R}^{N\times N}$ is the *graph Laplacian* [11]. From now on, we will assume that L always corresponds to a connected graph. We have the following lemma.

Lemma 1. *Let Γ and B be diagonal matrices as before, and assume that $\Gamma > 0$ (i.e., it is positive definite). Then*

$$\dim\Big[\mathscr{R}^\perp\big((\Gamma L) \otimes I_2 - (BL) \otimes S\big)\Big] = 2.$$

Proof. It suffices to show[2] that $\operatorname{null}[((\Gamma L) \otimes I_2 - (BL) \otimes S)^\mathsf{T}] = 2$. Notice now that $\operatorname{null}[(L\Gamma) \otimes I_2 + (LB) \otimes S)] = \operatorname{null}[(L \otimes I_2)(\Gamma \otimes I_2 + B \otimes S)]$. The matrix $\Gamma \otimes I_2 + B \otimes S$ is always invertible if $\Gamma > 0$. The result now follows from the fact that, for a connected graph, the Laplacian has a single eigenvalue at the origin [4], and hence $\operatorname{null}[L \otimes I_2] = 2$. □

Let $\mathbf{1}_N \stackrel{\text{def}}{=} (1, 1, \ldots, 1)^\mathsf{T} \in \mathbb{R}^N$ denote the N-dimensional column vector of ones, and recall that $L\mathbf{1}_N = 0$ [11, 4]. For any $v \in \mathbb{R}^2$ we have that

$$\big((\Gamma L) \otimes I_2 - (BL) \otimes S\big)(\mathbf{1}_N \otimes v) = (\Gamma L\mathbf{1}_N) \otimes v - (BL\mathbf{1}_N) \otimes (Sv) = 0. \tag{10}$$

Since $\operatorname{null}[(\Gamma L) \otimes I_2 - (BL) \otimes S] = 2$ it follows that $\mathbf{1}_N \otimes v$ spans to the null space of the matrix in (9). It follows that the equilibrium point $\bar{x}_\infty$ of (9) satisfies the condition $\bar{x}_\infty \stackrel{\text{def}}{=} \lim_{t\to\infty} x(t) = \mathbf{1}_N \otimes x_\infty$ for some $x_\infty \in \mathbb{R}^2$, equivalently, $\lim_{t\to\infty} x_1(t) = \lim_{t\to\infty} x_2(t) = \cdots = \lim_{t\to\infty} x_N(t) = x_\infty$.

The coordinates of the final consensus point $x_\infty = [\mathsf{x}_\infty\ \mathsf{y}_\infty]^\mathsf{T} \in \mathbb{R}^2$ can be explicitly computed using the following proposition.

Proposition 1. *Let $v_1, v_2 \in \mathbb{R}^{2N}$ be such that* $\operatorname{span}\{v_1, v_2\} = \mathscr{R}^\perp\big((\Gamma L) \otimes I_2 - (BL) \otimes S\big)$. *The final rendezvous point is given by*

$$x_\infty = \begin{bmatrix}\mathsf{x}_\infty \\ \mathsf{y}_\infty\end{bmatrix} = \begin{bmatrix}v_1^\mathsf{T}(\mathbf{1}_N \otimes I_2) \\ v_2^\mathsf{T}(\mathbf{1}_N \otimes I_2)\end{bmatrix}^{-1} \begin{bmatrix}v_1^\mathsf{T}x(0) \\ v_2^\mathsf{T}x(0)\end{bmatrix}. \tag{11}$$

[2] Here $\operatorname{null} A$ denotes the nullity of A, i.e., the dimension of the null space of the matrix A, that is, $\operatorname{null} A \stackrel{\text{def}}{=} \dim[\mathscr{N}(A)]$.

Proof. From Lemma 1 there exist linearly independent vectors $v_1, v_2 \in \mathscr{R}^{\perp}\big((\Gamma L)\otimes I_2 - (BL)\otimes S\big)$ such that $v_i^{\mathsf{T}}\dot{x} = -v_i^{\mathsf{T}}\big((\Gamma L)\otimes I_2 - (BL)\otimes S\big)x = 0$, $(i = 1,2)$. Consequently, $v_i^{\mathsf{T}}x(t) = v^{\mathsf{T}}x(0)$ for all $t \geq 0$. In particular, we have that $v_i^{\mathsf{T}}(\mathbf{1}_N \otimes x_\infty) = v_i^{\mathsf{T}}(\mathbf{1}_N \otimes I_2)x_\infty = v_i^{\mathsf{T}}x(0)$ $(i = 1,2)$. It follows that

$$\begin{bmatrix} v_1^{\mathsf{T}}x(0) \\ v_2^{\mathsf{T}}x(0) \end{bmatrix} = \begin{bmatrix} v_1^{\mathsf{T}}(\mathbf{1}_N \otimes I_2) \\ v_2^{\mathsf{T}}(\mathbf{1}_N \otimes I_2) \end{bmatrix} \begin{bmatrix} \mathsf{x}_\infty \\ \mathsf{y}_\infty \end{bmatrix} = \left(\begin{bmatrix} v_1^{\mathsf{T}} \\ v_2^{\mathsf{T}} \end{bmatrix} (\mathbf{1}_N \otimes I_2) \right) \begin{bmatrix} \mathsf{x}_\infty \\ \mathsf{y}_\infty \end{bmatrix}. \tag{12}$$

Since the vectors v_1 and v_2 are linearly independent, $\operatorname{rank}[v_1\, v_2] = 2$. Furthermore, $\operatorname{rank}(\mathbf{1}_N \otimes I_2) = (\operatorname{rank}\mathbf{1}_N)(\operatorname{rank} I_2) = 2$. Let now $\Theta \stackrel{\text{def}}{=} (\Gamma L)\otimes I_2 - (BL)\otimes S$. From the definition of v_1 and v_2, it follows that $\mathscr{N}\big(\begin{bmatrix} v_1\, v_2 \end{bmatrix}^{\mathsf{T}}\big) = \mathscr{R}(\Theta)$. An easy calculation also shows that $\mathscr{R}(\mathbf{1}_N \otimes I_2) = \mathscr{N}(\Theta)$ (refer also to equation (10)). Furthermore, one can easily show, along the lines of the proof of Lemma 1, that $\operatorname{rank}\Theta = \operatorname{rank}\Theta^2$, which implies that $\mathscr{R}(\Theta)\cap\mathscr{N}(\Theta) = \{0\}$. It follows immediately that $\mathscr{N}\big(\begin{bmatrix} v_1\, v_2 \end{bmatrix}^{\mathsf{T}}\big)\cap\mathscr{R}(\mathbf{1}_N \otimes I_2) = \{0\}$. Fact 2.10.14 in [2] yields that the 2×2 matrix in (12) has rank 2 and hence it is invertible. The result now follows directly from (12). □

Applications to Agent Orbit Design

In this section we investigate how several choices of the gain matrices Γ and B can generate specific patterns for the agent paths. Since we are mainly interested in periodic or quasi-periodic trajectories, we assume that $\Gamma = 0$. It follows that the closed loop system is given by

$$\dot{x} = ((BL)\otimes S)\,x. \tag{13}$$

It can be easily shown that the eigenvalues of BL are all real, hence the eigenvalues of the closed-loop matrix in (13) all lie on the imaginary axis. The structure of the corresponding state matrix in (13) (e.g., its eigenvalues and eigenvectors) can provide a great deal of information regarding the paths followed by the agents in the Cartesian coordinate frame, as well as the relative location of the agents on these paths (i.e., their relative phasing). For instance, one can ensure that the agent trajectories either form closed paths with given phasing, or they form a dense set of trajectories, ensuring that almost every point in a given region will be visited at least once by one or more agents.

Remark 3. In [15] Ren introduced Cartesian coupling in the consensus control law using a multiplication of the Laplacian matrix by a rotation matrix; this is similar to the skew-symmetric matrix we use in (13). Nonetheless, additional constraints on the Laplacian matrix are needed in [15] to capture the richness of trajectories we can obtain with the approach proposed in the current paper.

Case Study: Three Agents Connected in a Path Graph

In order to keep the analysis manageable, and to be able to provide closed-form expressions, henceforth we will restrict the discussion to three agents in the plane, that is, we take $N = 3$. For simplicity, we will also assume that the simplest agent interconnection topology, namely a path graph. The corresponding incidence matrix is given by

$$D = \begin{bmatrix} -1 & 0 \\ 1 & -1 \\ 0 & 1 \end{bmatrix}. \tag{14}$$

We are primarily interested in three types of closed curves: ellipses, epitrochoids, and hypotrochoids. Since the ellipses (and circles) have well-known parameterizations, next we will briefly review the main facts on epitrochoids and hypotrochoids. All these follow under the general class of *trochoid* curves, which includes cardioids, astroids, limaçons, and all polar coordinate roses [5].

An *epitrochoid* curve is generated by a point P attached at a radial distance d from the center of a circle of radius r, which is rolling without slipping around a circular track of radius R with angular velocity ω (see Fig. 1(a)). The distance d can be smaller, equal, or greater than the radius r of the rolling circle. In terms of Cartesian coordinates, an epitrochoid can be expressed as [8]

$$\mathsf{x}(\theta) = \mathsf{x}_c + (k+1)r\cos(\theta - \phi_A) - d\cos((k+1)\theta - \phi_B), \tag{15a}$$
$$\mathsf{y}(\theta) = \mathsf{y}_c + (k+1)r\sin(\theta - \phi_A) - d\sin((k+1)\theta - \phi_B), \tag{15b}$$

where ϕ_A and ϕ_B are constant angles, x_c and y_c are the coordinates of the center of the circular track of radius R and $k = R/r$. The angle θ denotes the angular position of the circle of radius r, given by $\theta = \omega t$. It can be shown that k is the number of points at which the agent is closest to the center of the circular track. For the purposes of this paper, we will henceforth refer to these points as *crests*. In the special case when $r = d$, the curve becomes an *epicycloid* with k cusps; at these points, the curve is not differentiable. Note that ellipsoidal paths correspond to the case when $k = 0$.

Another relevant curve of interest in this paper is the *hypotrochoid* [8], with parametric equations

$$\mathsf{x}(\theta) = \mathsf{x}_c + (k-1)r\cos(\theta - \phi_A) + d\cos((k-1)\theta - \phi_B), \tag{16a}$$
$$\mathsf{y}(\theta) = \mathsf{y}_c + (k-1)r\sin(\theta - \phi_A) - d\sin((k-1)\theta - \phi_B), \tag{16b}$$

where $k > 1$ with $k = R/r$ as before. The hypotrochoid can be reproduced by a point P attached at a distance d from the center of a circle of radius r, which rolls *inside* a circle of radius R. Again, the distance d can be smaller, equal, or greater than the radius r of the rolling circle; this radius, however, cannot exceed that of the circle R. Examples of hypotrochoids are shown in Fig. 1(b).

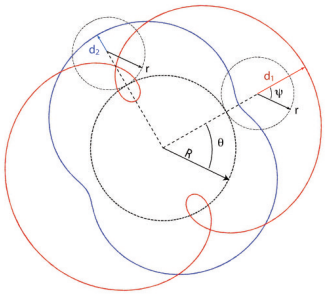

(a) Epitrochoid curves. The blue curve has $d < r$, while the second one has $d > r$. Both epitrochoids have $R = 4$, $r = 2$ (hence $k = 2$).

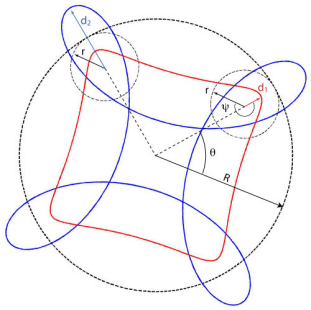

(b) Hypotrochoid curves. The blue curve has $d > r$, while the second one has $d < r$. Both hypotrochoids have $R = 6$, $r = 1.5$ (hence $k = 4$).

Fig. 1 Representative examples of epitrochoids and hypotrochoid curves.

Case I: Epitrochoidal Paths

Consider the case when $\Gamma = 0$ and $B = \mathrm{diag}(\beta, \beta, \beta)$, where $\beta > 0$. Following (9), the solution of the closed loop system can be obtained easily as follows

$$x(t) = \begin{bmatrix} \frac{1}{2}\sqrt{c_1^2 + c_2^2}\cos(\beta t - \phi_{12}) + \frac{1}{6}\sqrt{c_3^2 + c_4^2}\cos(3\beta t - \phi_{34}) + \frac{1}{3}c_5 \\ -\frac{1}{2}\sqrt{c_1^2 + c_2^2}\sin(\beta t - \phi_{12}) - \frac{1}{6}\sqrt{c_3^2 + c_4^2}\sin(3\beta t - \phi_{34}) + \frac{1}{3}c_6 \\ \hdashline \frac{1}{3}\sqrt{c_3^2 + c_4^2}\cos(3\beta t - \phi_{34}) + \frac{1}{3}c_5 \\ -\frac{1}{3}\sqrt{c_3^2 + c_4^2}\sin(3\beta t - \phi_{34}) + \frac{1}{3}c_6 \\ \hdashline -\frac{1}{2}\sqrt{c_1^2 + c_2^2}\cos(\beta t - \phi_{12}) + \frac{1}{6}\sqrt{c_3^2 + c_4^2}\cos(3\beta t - \phi_{34}) + \frac{1}{3}c_5 \\ \frac{1}{2}\sqrt{c_1^2 + c_2^2}\sin(\beta t - \phi_{12}) - \frac{1}{6}\sqrt{c_3^2 + c_4^2}\sin(3\beta t - \phi_{34}) + \frac{1}{3}c_6 \end{bmatrix}, \quad (17)$$

where $x_i = [\mathsf{x}_i \ \mathsf{y}_i]^\intercal \in \mathbb{R}^2$ for $i = 1, 2, 3$ and where $c_1, \ldots, c_6$ are constants depending on the initial conditions, and $\phi_{12} = \arctan(c_2/c_1)$ and $\phi_{34} = \arctan(c_4/c_3)$. Comparing the expressions for the $\mathsf{x}(\theta)$ and $\mathsf{y}(\theta)$ components of an epitrochoid in (15) to those in (17), the following observations can be made. First, for all agents, the center of their trajectories has coordinates $(\mathsf{x}_c, \mathsf{y}_c) = (\frac{1}{3}c_5, \frac{1}{3}c_6)$, which is the centroid of the initial positions of the agents. For agents no. 1 and no. 3, we have that $R_i + r_i = \frac{1}{2}(c_1^2 + c_2^2)^{\frac{1}{2}}$ and $d_i = \frac{1}{6}(c_3^2 + c_4^2)^{\frac{1}{2}}$ $(i = 1, 3)$. For the same two agents, $k = 2$, which implies that $R_i = 2r_i$ $(i = 1, 3)$. In other words, for any given initial positions, the ratio of the radius of the rolling circle to the radius of the track is fixed. Moreover, from the definition of k, it becomes evident that these two agents will describe epitrochoids with only two crests. The times at which agent no. 1 is closest and farthest from the center of its trajectory (its crests) can be computed from the solutions

of the equation

$$\sin(2\beta t - \phi_{12} + \phi_{34}) = 0. \tag{18}$$

Also, by considering the distance of the radius of agent no. 2 from the origin, it can be easily shown that the points of closest approach for agents no. 1 and no. 3 differ by an angle $\pi/2$ with respect to the center of the circular track. This relationship, along with (18), can be employed to calculate the orientation of the curves with respect to an absolute Cartesian coordinate frame. Agent no. 2 describes a circle of radius $R_2 = \frac{1}{3}(c_3^2 + c_4^2)^{\frac{1}{2}}$ with frequency 3β.

To demonstrate these facts, consider the case $B = \mathrm{diag}(1,1,1)$ with initial positions $x_1(0) = (6,8)$, $x_2(0) = (-7,5)$, $x_3(0) = (5,-10)$. The center of the orbits is located at $(\mathsf{x}_c, \mathsf{y}_c) = (0.33, 1.33)$. The radii of the circular tracks for agents no. 1 and no. 3 are $R_1 = R_3 = 2.40$, and the radii of the rolling circles for agents no. 1 and no. 3 are $r_1 = r_3 = 1.20$. The radius of the circle described by agent no. 2 is $R_2 = 1.49$. After computing the phase angles ϕ_{12} and ϕ_{34}, and evaluating

$$\delta = \arctan\left(\frac{\mathsf{y}_1(\tau) - \mathsf{y}_c}{\mathsf{x}_1(\tau) - \mathsf{x}_c}\right), \tag{19}$$

where τ is the solution of (18), it is found that the angle by which the crests of the epitrochoids are inclined with respect to the x-axis is $\delta = -18.81^\circ$. The corresponding trajectories are shown in Fig. 2.

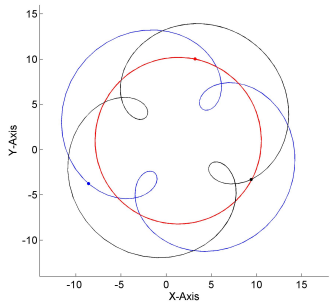

Fig. 2 Three agents displaying a circle and two epitrochoids when $B = \mathrm{diag}(1,1,1)$. The trajectory of agent no. 1 is shown in blue, the one of agent no. 2 is red, and the one of agent no. 3 in black.

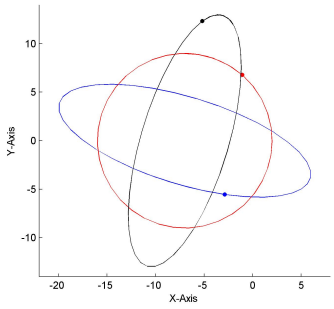

Fig. 3 Three agents displaying a circle and two ellipses when $B = \mathrm{diag}(1,-1,1)$. Again agent 1 is shown in blue, agent 2 in red, and agent 3 in black.

Case II: Ellipsoidal Paths

Consider now the case of the same system as before, but this time with the gains given as follows $B = \mathrm{diag}(\beta, -\beta, \beta)$, where $\beta > 0$. The solution of the closed-loop

system in this case leads to

$$x(t) = \begin{bmatrix} c_2 \sin\beta t + c_3 \cos\beta t + c_5 \\ -c_1 \sin\beta t + c_4 \cos\beta t + c_6 \\ (c_2 - c_4)\sin\beta t + (c_3 - c_1)\cos\beta t + c_5 \\ (c_3 - c_1)\sin\beta t + (c_4 - c_2)\cos\beta t + c_6 \\ -c_4 \sin\beta t - c_1 \cos\beta t + c_5 \\ c_3 \sin\beta t - c_2 \cos\beta t + c_6 \end{bmatrix}, \tag{20}$$

where as before $c_1, \ldots, c_6$ are constants depending on the initial conditions. The trajectories of agents no. 1 and no. 3 are ellipses, while that of agent no. 2 is a circle. All three trajectories are centered around the point with coordinates $(\mathsf{x}_c, \mathsf{y}_c) = (c_5, c_6)$ and all of them have a period $T = 2\pi/\beta$. Furthermore, it is easy to show that the trajectory of agent no. 3 is an ellipse geometrically identical to that of agent no. 1, but rotated $\pi/2$ radians in the counterclockwise direction. The second observation is that whenever agent no. 1 is at the tip any of its semi-major axis, agent no. 3 is at the tip of its semi-minor axis, and vice-versa. The radius of the circle described by agent no. 2 is $R_2 = \sqrt{(c_1 - c_3)^2 + (c_2 - c_4)^2}$. Analytical expressions for the semi-major and semi-minor axes of the ellipses described by agents no. 1 and no. 3 can be computed by solving for the times at which the distance from the origin is at a maximum and at a minimum. Note that ellipses are special cases of hypotrochoids with $R = 2r$. Figure 3 shows an example for this scenario with $B = \mathrm{diag}(1, -1, 1)$ and initial conditions $x_1(0) = (-12, -3)$, $x_2(0) = (-7, 9)$, $x_3(0) = (-2, 12)$.

Case III: Hypotrochoidal Paths

Consider now the case when $B = \mathrm{diag}(\beta, \beta, -\beta)$, where $\beta > 0$. The analytic calculation of the solution is cumbersome and is omitted for the sake of brevity. Instead, insightful conclusions about the ensuing paths can be drawn by investigating the eigenvalues of the state matrix. A simple calculation shows that the nonzero eigenvalues of the matrix $(BL) \otimes S$ are $\lambda_{1,2} = \pm\beta(\sqrt{2} - 1)\mathrm{i}$ and $\lambda_{3,4} = \pm\beta(\sqrt{2} + 1)\mathrm{i}$. From the expression $\beta(\sqrt{2} + 1) = (k - 1)\beta(\sqrt{2} - 1)$ it follows

$$\frac{R - r}{r} = k - 1 = \frac{1 + \sqrt{2}}{\sqrt{2} - 1}. \tag{21}$$

It follows that the number of crests is given by $k = 4 + 2\sqrt{2} \cong 6.83$, which is an irrational number. A general result in analytic geometry [8] states that if k is irrational, then the number of crests described by the hypotrochoid is infinite. The curve does not close, and the trajectories form a dense subset of the space between the bounding circle R and the circle of radius $R - 2r$. In other words, as $t \to \infty$, the hypotrochoids described by each of the three agents fill annular areas.

The following expressions for the radius of the rolling circle r_i and the distance d_i to the point P can be derived for the three agents. These can be used to obtain the solution in terms of phase-angle relationships. Figure 4(a) shows an example with

$B = \mathrm{diag}(1,1,-1)$ and initial conditions $x_1(0) = (8,-7),\ x_2(0) = (0,6),\ x_3(0) = (12,14)$.

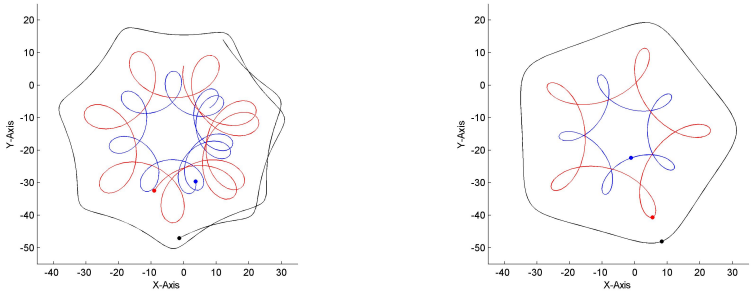

(a) A set of three hypotrochoids described by three agents. Although each one has a different r_i, d_i and R_i parameters, they all display non-closing curves. Notice that the value of k for this example is irrational.

(b) Same group of agents as in (a), with control redesign to describe closed hypotrochoids with five crests. This pattern necessitates a different graph topology of the intra-agent information exchange (i.e., a cycle graph).

Fig. 4 Examples of hypotrochoidal paths with three agents interconnected in a path graph and a cycle graph.

General Case

The system (13) describe a rich family of geometric curves. However, this is still restrictive in the sense that the curves have some fixed parameters that cannot be altered by just changing the initial conditions. For instance, the epitrochoids described in Case I can only have two crests. Moreover, the orbits of agents no. 1 and no. 3 are identical, except for the fact that they are phased apart by an angle $\pi/2$, along with the condition that the trajectory of agent no. 2 is a circle. Similar statements can be made for Cases II and III. Also, recall that the hypotrochoids of Case III were not periodic. It would be of great interest to a mission designer to be able to employ vehicles generating in a distributed, cooperative manner suitable trajectories with specific geometric characteristics. For instance, it may be desirable to be able generate epitrochoids or hypotrochoids with a certain number of crests in order to survey an area or perimeter of interest, or provide telecommunication coverage over a region, etc.

Based on the discussion in the previous sections, the shape and frequencies of the resulting paths/trajectories is determined by the eigenvalues and eigenvectors of the matrix $(BL) \otimes S$. Recall from the properties of the Kronecker product that the eigenvalues of the matrix $(BL) \otimes S$ are of the form $\lambda\mu$ where $\lambda \in \mathrm{spec}(BL)$ and $\mu \in \mathrm{spec}\, S$. Additionally, the corresponding eigenvectors are of the form $\mathsf{v} \otimes \mathsf{u}$ where $\mathsf{v} \in \mathbb{C}^3$ is the eigenvector of the matrix BL associated with λ and $\mathsf{u} \in \mathbb{C}^2$ is the eigenvector

of the matrix S associated with μ. The task of agent trajectory design therefore reduces to the task of imposing the correct conditions on the spectral properties of the matrix BL. For example, closed paths with the correct number of crests may be ensured by selecting a suitable rational value of k, along with the eigenvalues of the matrix BL. The type of path (epitrochoid, ellipse, hypotrochoid) may be determined by the corresponding eigenvectors. It is clear that the path design depends both on the feedback gain matrix B, as well as on the imposed graph topology represented by the incident matrix D (equivalently, the graph Laplacian L).

Consider, for instance, again Case III of hypotrochoidal paths shown in Fig. 4(a), and let us assume that we want to keep the general, overall shape of these paths, but we want to have closed, periodic paths instead with a given number of crests. By keeping the same eigenvectors and by changing only the eigenvalues (choose for instance the smallest nonzero eigenvalue to be equal to $\lambda_{1,2} = 5/3$) and by imposing five crests (hence $k = 5$), we are led to the following control law[3]

$$u = ((B \circ D) \otimes S)z = ((B \circ D) \otimes S)(D^{\mathsf{T}} \otimes I_2)x, \tag{22}$$

which can be written, componentwise, as follows

$$u_i = \sum_{k=1}^{M} \beta_{ik} d_{ik} p_k = \sum_{k=1}^{M} \beta_{ik} d_{ik} S z_k, \quad i = 1, \ldots, N, \tag{23}$$

where $B = \begin{bmatrix} 0.6213 & 0.8431 & 0.1109 \end{bmatrix} \otimes \begin{bmatrix} 1 & 1 & -1 \end{bmatrix}^{\mathsf{T}}$ and with an incidence matrix

$$D = \begin{bmatrix} -1 & 0 & 1 \\ 1 & -1 & 0 \\ 0 & 1 & -1 \end{bmatrix}. \tag{24}$$

The trajectories of the agents are shown in Fig. 4(b). Note that these trajectories necessitate a different communication topology, namely, one which, for this case, corresponds to a complete graph.

Conclusions

We have presented an extension of the classical consensus algorithm for multi-agent systems. The main idea hinges on the use, by each agent, of additional directional information that can be readily inferred from knowledge of the relative position with respect to the other agents. The resulting control law seems to be a genuine generalization of the classical consensus design protocol since it is not induced by a scalar potential, and it can lead to agreement values that lie outside the convex hull of initial conditions. A special choice of the feedback gains leads to periodic or quasi-periodic solutions that can be used to design trajectories suitable for persistent optimized surveillance and monitoring applications by a team of agents. The result-

[3] Recall that, given two matrices $A \in \mathbb{R}^{n \times m}$ and $B \in \mathbb{R}^{n \times m}$ the Schur product $A \circ B$ is defined by $(A \circ B)_{ij} = A_{ij} B_{ij}$.

ing trajectories show intricate geometric patterns generated using only relative, local information. Future work will concentrate on developing a general theory for orbit synthesis for an arbitrary number of agents in two and three dimensions.

References

1. Arcak, M.: Passivity as a design tool for group coordination. IEEE Transactions on Automatic Control **52**(8), 1380–1390 (2007)
2. Bernstein, D.S.: Matrix Mathematics: Theory, Facts, and Formulas, 2nd edn. Princeton University Press, Princeton, New Jersey (2009)
3. Fax, J.A., Murray, R.M.: Information flow and cooperative control of vehicle formations. IEEE Transactions on Automatic Control **49**(9), 1465–1476 (2004). DOI 10.1109/TAC.2004.834433
4. Godsil, C., Royle, G.: Algebraic Graph Theory. Springer New York (2001)
5. Hall, L.: Trochoids, Roses, and Thorns–Beyond the Spirograph. College Mathematics Journal **23**(1), 20–35 (1992)
6. Justh, E., Krishnaprasad, P.: Equilibria and Steering Laws for Planar Formations. Systems & Control Letters **52**(1), 25–38 (2004). DOI 10.1016/j.sysconle.2003.10.004
7. Justh, E.W., Krishnaprasad, P.S.: Natural frames and interacting particles in three dimensions. In: Proc. and 2005 European Control Conf. Decision and Control CDC-ECC '05. 44th IEEE Conf, pp. 2841–2846 (2005)
8. Lawrence, J.: A Catalog of Special Plance Curves, first edn. Dover Publications (1972)
9. Leonard, N.E., Fiorelli, E.: Virtual leaders, artificial potentials, and coordinated control of groups. Proc. of the 40th IEEE Conference on Decision and Control pp. 2968–2973 (2001)
10. Marshall, J.A., Broucke, M.E., Francis, B.A.: Formations of vehicles in cyclic pursuit. IEEE Trans. on Automatic Control **49**(11), 1963–1974 (2004)
11. Mesbahi, M., Egerstedt, M.: Graph Theoretic Methods in Multiagent Networks. Princeton University Press, Princeton, New Jersey (2010)
12. Olfati-Saber, R., Fax, J.A., Murray, R.M.: Consensus and cooperation in multi-agent networked systems. Proceedings of the IEEE **97**, 215–233 (2006)
13. Olfati-Saber, R., Murray, R.M.: Consensus problems in networks of agents with switching topology and time-delays. IEEE Trans. on Automatic Control **49**(9), 1520–1533 (2004)
14. Pavone, M., Frazzoli, E.: Decentralized policies for geometric pattern formation and path coverage. Journal of Dynamic Systems, Measurement, and Control **129**, 633–643 (2007). DOI 10.1115/1.2767658
15. Ren, W.: Collective motion from consensus with cartesian coordinate coupling - part i: Single-integrator kinematics. In: Proc. 47th IEEE Conf. Decision and Control CDC 2008, pp. 1006–1011 (2008). DOI 10.1109/CDC.2008.4738708
16. Ren, W., Beard, R.W.: Consensus seeking in multi-agent systems using dynamically changing interaction topologies. IEEE Trans. on Automatic Control **50**(5), 655–661 (2005). DOI 10.1109/TAC.2005.846556
17. Scardovi, L., Leonard, N.E., Sepulchre, R.: Stabilization of collective motion in three dimensions: A consensus approach. In: Proc. 46th IEEE Conf. Decision and Control, pp. 2931–2936 (2007). DOI 10.1109/CDC.2007.4434721
18. Sepulchre, R., Paley, D.A., Leonard, N.E.: Stabilization of planar collective motion: All-to-all communication **52**(5), 811–824 (2007). DOI 10.1109/TAC.2007.898077
19. Singh, L., Stephanou, H., Wen, J.: Real-time robot motion control with circulatory fields. In: 1996 IEEE International Conference on Robotics and Automation, 1996. Proceedings., pp. 2737–2742 (1996)
20. Suzuki, I., Yamashita, M.: Distributed anonymous mobile robots: Formation of geometric patterns. SIAM J. on Computing **28**(4), 1347–1363 (1999)
21. Wang, L.S., Krishnaprasad, P.S.: Gyroscopic control and stabilization. Journal of Nonlinear Science **2**, 367–415 (1992)